while B varied only ± 0.2 about its 11.2 kMc value of 5.8.

For twists of less than 70° a remains constant, while the approximation that B is a constant degenerates; for twists of more than 80° the approximation that a is a constant apparently degenerates, while the approximation that B is a constant improves.

At first glance the apparent 22 per cent error in assuming a equal to a constant for the 80° twist might appear alarming, but it should be remembered that this 22 per cent error is measured over a 1000-Mc range, whereas the 80° twist can be utilized in a filter cavity to produce no more than a 30-Mc bandwidth filter. Actually at the 3-db points, a differs from the 11.2 kMc value by less than 1 per cent. The approximation that a is a constant thus remains valid for twist angles greater than 80°, as well as for twist angles less than 70°.

The approximation that B is a constant, while being very good at twist angles of 80° and higher, is beginning to degenerate for a 70° twist. It is expected that, due to this variation, the design formulas will degenerate for bandwidths much in excess of 10 per cent.

ACKNOWLEDGMENT

The author would like to express his thanks to S. F. Jankowski and J. D. Deith for experimental assistance, and to D. H. Ring, E. A. Marcatili, and others at the Holmdel laboratory for many informative discussions.

Resonators for Millimeter and Submillimeter Wavelengths*

WILLIAM CULSHAW†, SENIOR MEMBER, IRE

Summary—**Further considerations on the mm-wave Fabry-Perot interferometer are presented. Computed Q values for parallel metal plate resonators indicate that at spacings around 2.5 cm, values ranging from 60,000 at 3 mm, to 300,000 at 0.1 mm wavelengths are possible. The plates must, however, be quite flat. These results are important for many investigations, and in particular for mm and sub-mm wave maser research. For the aperture per wavelength ratios possible here, diffraction effects should be small. Consideration is given to using curved reflectors or focused radiation in applications where the fields must be concentrated. For this purpose, re-entrant conical spherical resonators are treated in detail, as regards operation in the TEM mode at high orders of interference. Expressions for the Q and shunt impedance are given, and high values are possible at mm and sub-mm wavelengths. Quasi-optical methods of coupling into and out of such a resonator are proposed, and the higher modes possible in such a resonator are considered. Results indicate that it could have application to the mm-wave generation problem, and that it represents a good resonant cavity for solid state research at mm and sub-mm wavelengths, and for maser applications in particular.**

INTRODUCTION

IN the region of wavelengths extending downwards from around 1 mm to the long infrared, much important research needs to be done, and many important applications arise. At these wavelengths, conventional cavity resonators become extremely minute, since their dimensions are around one-half wavelength. For some purposes, cavities of larger dimensions, capable of sustaining a number of higher order modes, are possible. This is a difficult procedure, and the difficulties increase with decreasing wavelength for a given size of cavity. Cavities much larger in terms of the wavelength, but which permit mode-free operation, are thus needed. In particular, the development of such a cavity with a suitable interaction gap and new methods of input and output coupling other than conventional waveguides would greatly assist in the development of a primary coherent electronic source for these wavelengths.

Referring to the reflex klystron, which for many purposes is still the most versatile and simplest of microwave tubes, such a cavity must be capable of bunching the electron stream, and hence must possess a suitable interaction gap of small dimensions compared to the wavelength. It also should have a large resonator volume for heat dissipation and a high shunt impedance for efficient electronic interaction. New methods for coupling into and out of the resonator are also necessary. There are other problems, as well, in the design of such tubes for very short wavelengths; another very important one being the provision of an adequate current density at these short wavelengths where the area of the electron beam for efficient interaction with the resonator steadily decreases. This difficulty would certainly be helped by providing larger, more efficient, and more suitable resonators. The required current densities in the resonator gap could possibly be approached with improved cathodes and by the use of suitable magnetic or

* Received by the PGMTT, July 8, 1960; revised manuscript received, October 31, 1960.
† Natl. Bur. of Standards, Boulder Labs., Boulder, Colo.

other focusing devices. In any event, such a resonator development would permit the extension of klystron techniques to shorter wavelengths, and could lead to easier construction techniques and higher powers from tubes presently available at wavelengths extending from 8 mm to around 2.5 mm.

Some progress in this general direction was effected by the development of the dielectric tube resonator.[1] This was used to produce interaction with highly bunched electron beams traveling at relativistic velocities.[2] Such cavities, however, are still not large enough in terms of the wavelength, they do not possess high enough Q values for many purposes, and their use would seem to be limited. Another possibility which seems to possess considerable potential for application in all areas of mm wave research is the mm-wave Fabry-Perot interferometer.[3,4] While this form of resonator is eminently suitable for many purposes, there are other applications, such as the electronic generation problem, or solid-state research, for which a smaller interaction space is desirable. Thus one might make the reflectors spherical and use focused radiation between them. Here diffraction problems arise,[5] and while such a system should resonate at infrared or shorter wavelengths, it may not do so at longer mm wavelengths, unless it is large. In any event, it is difficult to confine the field into linear dimensions even of the order of a wavelength in extent, and such a degree of confinement is not sufficient for the efficient bunching of electron streams as in a klystron. Thus, one must consider the provision of side walls round the interferometer, and a deformation of this into a cavity resonator bounded by two re-entrant cones and a sphere. Such a cavity was considered in the classical paper by Hansen and Richtmeyer[6] on resonators suitable for klystron oscillators, and it has also received considerable attention, particularly by Schelkunoff,[7,8] in the treatment of biconical antennas. At longer wavelengths, other types of resonators proved more suitable. However, at mm and sub-mm wavelengths, such conventional resonators become very small and serious problems arise in heat dissipation, low Q factors, low shunt impedance and in fabrication.

The paper presents a new appraisal of the biconical spherical resonator in the light of the new developments in the mm-wave Fabry-Perot interferometer and the possibility of operating such a biconical resonator at large orders of interference. This would provide a suitable resonator for the purposes discussed above. Features which help this approach considerably are that the coupling into the large biconical resonator is possible by a whole series of regularly spaced coupling holes as in the mm-wave interferometer, and optical methods such as focusing may be used to get the radiation into and out of such a resonator. Such methods seem highly desirable in this wavelength region.

Planar Millimeter Wave Interferometer or Resonator

Fig. 1 shows the mm-wave interferometer as used in transmission measurements.[4] The reflector system may be regarded as a resonant cavity formed by the parallel metal plates and the multiple reflections of plane waves between them. The holes are then exactly analogous to the coupling holes or irises used in microwave cavity resonators, and they provide the means for coupling into and out of the resonance region between the plates, while preserving the large Q value of the metal plate region. For small holes, the loading on the interferometer due to the generator and load impedances is small and can be adjusted by the hole diameter. Side wall losses are essentially absent except for diffraction effects, which can be kept small, and which decrease with decreasing wavelength. This results in a Q for the interferometer which increases directly as the order of interference. Referring to Fig. 1, the field at resonance due to plane waves between the plates with the origin as shown is given by

$$E_y = -2jE_0 \sin (n\pi z/d),$$
$$\eta H_x = 2E_0 \cos (n\pi z/d), \tag{1}$$

where d is the distance between the plates, E_0 is a constant, and $\eta = (\mu/\epsilon)^{1/2}$ is the intrinsic impedance of the medium between the plates in mks units. The energy stored and the mean power lost per unit area of the plates may be deduced from (1), and hence the unloaded Q determined, *viz.*,

$$Q_0 = \lambda/\Delta\lambda = n\pi/(1 - R), \tag{2}$$

where $R = 1 - (8\epsilon\omega/\sigma)^{1/2}$ is the power-reflection coefficient of the metal, ϵ and μ are its permittivity and permeability, usually equal to those of free space, σ is the conductivity, and ω is the angular frequency. In terms of the fringe width Δd between half power points we may write, using the equation $2d = n\lambda$,

$$Q_d = \lambda/\Delta d = 2\pi/(1 - R). \tag{3}$$

[1] R. C. Becker and P. D. Coleman, "The dielectric tube resonator: a device for the generation and measurement of millimeter and submillimeter waves," *Proc. Symp. on Millimeter Waves*, Polytechnic Inst. of Brooklyn, Brooklyn, N. Y., pp. 191–222; March, 1959.

[2] M. D. Sirkis and P. D. Coleman, "The harmodotron—a megavolt electronics millimeter wave generator," *J. Appl. Phys.*, vol. 28, pp. 944–950; September, 1957.

[3] W. Culshaw, "Reflectors for a microwave Fabry-Perot interferometer," IRE Trans. on Microwave Theory and Techniques, vol. MTT-7, pp. 221–228; April, 1959.

[4] W. Culshaw, "High resolution millimeter wave Fabry-Perot interferometer," IRE Trans. on Microwave Theory and Techniques, vol. MTT-8, pp. 182–189; March, 1960.

[5] G. W. Farnell, "Measured phase distribution in the image space of a microwave lens," *Canad. J. Phys.*, vol. 36, pp. 935–943; July, 1958.

[6] W. W. Hansen and R. D. Richtmeyer, "On resonators suitable for klystron oscillators," *J. Appl. Phys.*, vol. 10, pp. 189–199; March, 1939.

[7] S. A. Schelkunoff, "Electromagnetic Waves," D. Van Nostrand Book Co., Inc., New York, N. Y., pp. 285–290; 1943.

[8] S. A. Schelkunoff, "Advanced Antenna Theory," John Wiley and Sons, Inc., New York, N. Y., pp. 32–71; 1952.

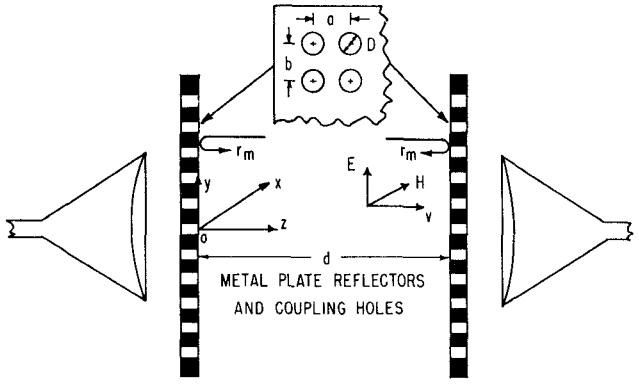

Fig. 1—Millimeter wave Fabry-Perot interferometer.

Since R will be around 0.999 for a metal at these frequencies, (3) shows that the metal plates must be quite flat, within 1/1000 of the operating wavelength.

Table I gives values of Q_0 for wavelengths extending into the submillimeter region and illustrates the great advantages of the Fabry-Perot interferometer, since it would be very difficult, if not impossible, to make conventional cavity resonators for these wavelengths. In contrast to these results, ideally an unloaded Q value of some 9000 would be obtained at 1 mm wavelength with a cylindrical cavity of diameter 0.060 inch operating in the $TE_{01,50}$ mode. This interferometer is thus ideal for many purposes, permitting the use of relatively large structures at these very short wavelengths with freedom from most higher order modes.

TABLE I

COMPUTED UNLOADED Q VALUES FOR SILVER PLATES SPACED 2.5 CM APART IN A MM-WAVE INTERFEROMETER (CONDUCTIVITY σ TAKEN AS 6.139×10^7 MHOS/M).

λ_{mm}	n	R	Q_0
3.125	16	0.99917	60,300
2.0	25	0.99896	75,300
1.0	50	0.99852	106,500
0.5	100	0.99792	150,000
0.1	500	0.99533	333,900

At suitable terminals, the holes may be regarded as perfect transformers, which enable us to couple into the metal plate resonator, in a uniform and efficient manner. Equivalent circuits for the mm-wave Fabry-Perot interferometer may now be drawn, and are shown in Fig. 2(a) and 2(b) for the transmission and reaction types respectively. The hole size may now be fixed by equating the reflectivity of the bulk metal to that deduced by regarding the hole as a reactive structure on a transmission line.[3] Smaller and larger hole sizes than those given by this criterion correspond respectively to lower and higher values of loading on the interferometer than those given by the matched condition. Such reflectors will have adequate bandwidth for mm-maser and spectroscopy applications, and designs can be optimized for any given wavelength region. The application of the

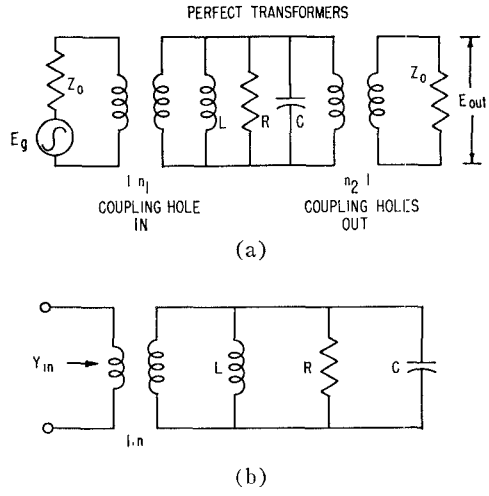

Fig. 2—Equivalent circuits for interferometer. (a) Transmission type. (b) Reaction type.

Fabry-Perot interferometer to the problem of mm-wave masers and spectroscopy is under active development.

CURVED OR FOCUSED FABRY-PEROT RESONATORS

For some experiments and applications, the planar type of interferometer or resonator is not suitable. Examples of this occur in solid-state research, optical-maser work, and electronic interaction with electric fields. Here, the resonator fields must be concentrated into a smaller volume, and it is natural to consider the use of cylindrical or spherical Fabry-Perot plates and focused radiation to produce concentrated fields in the vicinity of a focus. Such an arrangement might resonate in an analogous way to the plane reflector geometry, and coupling again be effected by a whole series of coupling holes. Fig. 3 shows a possible arrangement for a transmission interferometer employing curved reflectors. Either cylindrical or spherical reflectors could be used with appropriate lenses. The lines showing the concentration of the field and the constant-phase fronts are purely qualitative, but indicate approximately the field distribution between such plates.

The field distribution near the focus of a converging spherical wave has received extensive theoretical study.[9] With the coherent microwave sources and techniques now available, the field distribution in such regions can be experimentally determined. Such work has substantiated the results obtained by applying scalar diffraction theory to this problem when the aperture dimensions are some twenty wavelengths or more in extent,[5] and the regions of interest are close to the axis and somewhat distant from the lens. The literature on this subject is quite extensive, and we shall limit our remarks to those closely connected with the idea of using curved Fabry-Perot resonators.

[9] M. Born and E. Wolf, "Principles of Optics," Pergamon Press, London, Eng. pp. 434–448; 1959.

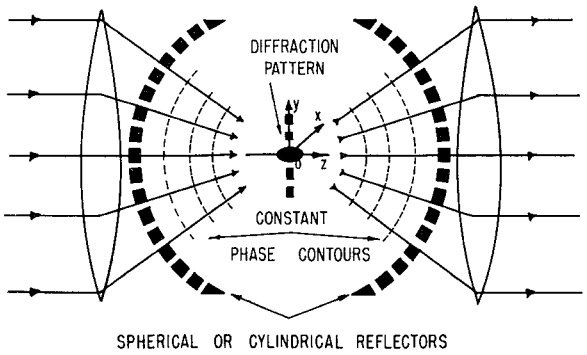

Fig. 3—Focused Fabry-Perot interferometer.

A full treatment of the problem for optics is given in reference 9, and general expressions are derived for the field in the focal region. Referring to Fig. 3, isophotes, or contour lines of intensity $I(p, q)$ near the focus of a converging spherical wave, as well as contours of equal phase, are given. Here $p=\beta z(a/f)^2$, and $q=\beta\rho(a/f)$, where $2a$ is the aperture diameter, f is the focal length, $\beta=2\pi/\lambda$, and $\rho=(x^2+y^2)^{1/2}$ is the radial distance in the focal plane $z=0$. In optics, the intensity distribution is symmetrical about the geometrical focal plane and also about the z axis. Also, the surfaces of constant phase are surfaces of revolution about the z axis. At a distance from the focus, the constant phase surfaces coincide with the spherical wave fronts of geometrical optics but become gradually deformed near the focal region. In the immediate region of the focus, the constant phase surfaces are plane, and on passing through this region, they gradually deform and again become spherical, but with opposite curvature.

In the focal plane $z=0$, the intensity is given by[9]

$$I(0, q) = \left[\frac{2J_1(q)}{q}\right]^2 I_0, \tag{4}$$

where J_1 is the usual Bessel function. This distribution is characteristic of the Airy-ring diffraction pattern in the image plane of an optical lens.[10] Along the z axis, the field intensity is given by

$$I(p, 0) = \left[\frac{\sin p/4}{p/4}\right]^2 I_0. \tag{5}$$

Eqs. (4) and (5) indicate the degree of confinement of the field possible in the focal region for given ratios of f/a. The first zero of $J_1(q)$ is at $q=3.83$; and for $f/a=4$, the radius to the zero of the central ring is 2.5λ. Along the z axis, the first zeros occur for $z=\pm f^2\lambda/2a^2$, and for $f/a=4$, we obtain $z=\pm 8\lambda$.

Farnell[5] discusses the field in the image space of a microwave lens, the main differences from optics arising because of the much smaller aperture to wavelength ratios possible with microwaves. With an optical lens, the field in the focal region is concentrated into smaller volumes and approximations can be used which are not necessarily valid for microwaves. Fig. 4 shows measured contours of constant phase in the image space of a microwave lens. This had a diameter of 50 cm, a focal length around 60 cm, and the wavelength used was 3.22 cm. Contours of constant intensity are also given in reference 5. The same general features discussed above for light optics are evident; there are, however, differences in the shape of the contours. Here the constant phase surfaces and the Airy pattern in the focal plane are slightly curved, the center of curvature being at the lens center as shown. Also the center of curvature of the wave diverging from the focus is at the position of maximum intensity which is not at the focus, but at a point some 2 wavelengths nearer the lens. The center of curvature of the converging wave, however, is at the geometrical image or focus. The deviations are due to the larger angular patterns which occur with microwave lenses, and at shorter mm and sub-mm wavelengths with similar aperture sizes, the optics distribution discussed above would be approached.

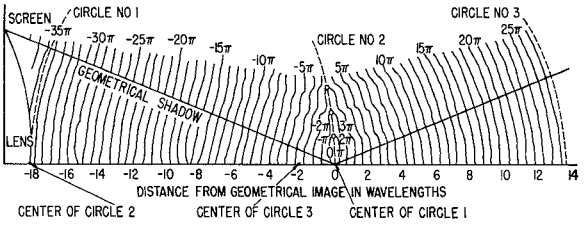

Fig. 4—Measure contours of constant phase in image space of a microwave lens with $R=63$ cm, $a=25$ cm, and $\lambda=3.22$ cm. Phase at geometrical image taken as $\pi/2$ radians. (After G. W. Farnell, *Canad. J. Phys.*, vol. 36, p. 935; 1958.)

Matthews and Cullen[11] have investigated at microwaves a converging spherical wave limited by a rectangular aperture. The approximations used in their analysis correspond to those used in optics, and are therefore valid when the diffraction pattern in the focal region is of small extent. Their deductions and measurements, however, give an interesting physical picture of what happens in the focal region and indicate that there are variations in axial wavelength in the focal region as compared to the free space wavelength. Results in the regions investigated indicated an increase in axial wavelength, or a decrease in the axial propagation constant at small distances either side of the focus. Linfoot and Wolf[12] also deduce that in optics there are regions very near the focus where the nearly plane constant phase surfaces are spaced closer together by a factor $1-a^2/4f^2$ than those in a parallel beam of light of the same wave-

[10] *Ibid.*, pp. 394–397.

[11] P. A. Matthews and A. L. Cullen, "A study of the field distribution at an axial focus of a square microwave lens," *Proc. IEE*, Pt. C., vol. 103, pp. 449–456; July, 1956.

[12] E. H. Linfoot and E. Wolf, "Phase distribution near focus in an aberration-free diffrasion image," *Proc. Phys. Soc. (London)*, vol 69, pp. 823–832; November, 1956.

length. There are also regions of rapid phase variation at the nulls of the Airy pattern and along the axis.

We may sum up the possible use of curved reflectors for the mm and sub-mm resonator problem as follows. A spherical or cylindrical converging wavefront limited by an aperture gives a region near the focus where the field is concentrated within distances of a few wavelengths. At optical wavelengths, spherical or cylindrical reflectors placed along appropriate phase contours on either side of the focus should resonate at the appropriate wavelength. As indicated by the work at wavelengths of 3.2 cm, there may be departures from ideal conditions at mm and sub-mm wavelengths, and no such resonance may be possible. The problem in this respect needs further investigation. Such resonator types could thus be useful in optical masers and possibly at very short mm wavelengths, although close attention to the preservation of phase shapes in the focal region when obstacles are inserted would be necessary. Since the field in the focal region is still some wavelengths in extent, such a resonator is not suitable for electron bunching or for harmonic extraction from bunched electron beams.

Biconical Spherical Resonators

A. Dimensions, Q Values and Shunt Impedance

The cavity resonator bounded by two re-entrant cones and a sphere, as shown in Fig. 5, was considered in the early phases of klystron resonator development and has also been considered by Schelkunoff.[7] These investigations were concerned with such spherical resonators of radius equal to $\lambda/4$ or with orders of interference of unity. The feature which makes a new appraisal worthwhile is that such resonators can be operated at higher orders of interference provided facilities exist for coupling into and out of such a resonator in a uniform way and no serious difficulties from higher order modes are encountered. Such a method is that of a whole series of coupling holes as used in the planar Fabry-Perot interferometer. Useful features of such a biconical resonator, especially at mm and sub-mm wavelengths, are that the resonator becomes larger, the Q increases with order of interference, and shunt impedance remains high.

Referring to Fig. 5, if an RF voltage is impressed between the apices of the cones, the principal or TEM mode on such a structure is generated. This has the electric lines coinciding with meridians and the magnetic lines along circles coaxial with the axis as shown. Such a system is equivalent to a transmission line of characteristic impedance given by

$$Z_c = 120 \log \cot (\psi/2), \tag{6}$$

and expressions for the electric and magnetic fields may be obtained.[7] Resonances occur when the radius lq of the spherical boundary is equal to $n\lambda/4$, where n is an integer referred to as the order of interference. Here we consider odd values of n or the case of parallel resonance.

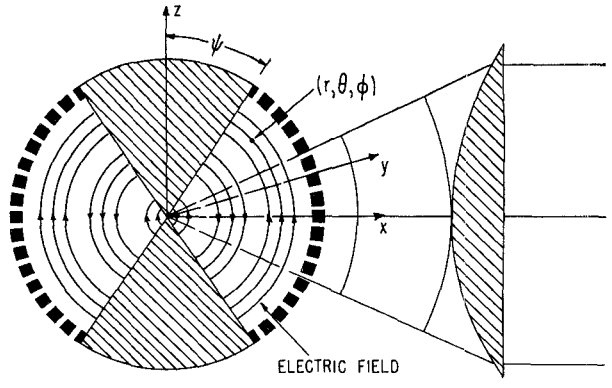

Fig. 5—Biconical spherical resonator and principal TEM mode.

Standing waves then exist in the resonator, and the Q value may be determined for any order n of interference. For equal and opposite cones in the sphere we thus obtain

$$Q_0 = \frac{30\pi^2 n \log \cot (\psi/2)}{R_m[\log \cot (\psi/2) + P \operatorname{cosec} \psi]}, \tag{7}$$

where ψ is the cone angle in Fig. 5 and R_m is the resistive part of the intrinsic impedance of the metal. The parameter P is given by

$$P = \tfrac{1}{2}[C + \log n\pi - Ci(n\pi)], \tag{8}$$

where C is Euler's constant, equal to 0.5772, and the function

$$Ci(x) = \int_{\infty}^{x} \frac{\cos t}{t}\, dt, \qquad x > 0. \tag{9}$$

Similarly, the shunt impedance at resonance is given by

$$Z_s = \frac{14400\pi[\log \cot (\psi/2)]^2}{R_m[\log \cot (\psi/2) + P \operatorname{cosec} \psi]}. \tag{10}$$

Apart from changes due to the increased order of interference n, (7) and (10) are similar to those given by Schelkunoff.[7]

For $n=1$, Q_0 is a maximum when $\psi = 33.5°$, and is equal to $132/R_m$; hence $Q_0 = 924$ for such a copper resonator at $\lambda = 1$ mm. Also, for $n=1$, Z_s is optimum when $\psi = 9.2°$ and equal to $3.74 \times 10^4/R_m$ ohms; hence for copper $Z_s = 2.6 \times 10^5$ ohms at $\lambda = 1$ mm. It is evident that such a resonator has a high shunt impedance even at short wavelengths, which is a desirable feature for a klystron resonator. However, for $n=1$, the diameter is around 0.020 inch and thus is not very practical. The Q is also low at short wavelengths for this small order of interference.

Fig. 6 shows curves of Q_0 and shunt impedance Z_s for a copper resonator at a wavelength of 1 mm and order of interference $n=41$. As for $n=1$, Q_0 is a maximum when $\psi = 33.5°$. The optimum angle for Z_s depends on n, and is given by

$$P \cot \psi - (2P \operatorname{cosec} \psi)/[\log \cot (\psi/2)] = 1. \tag{11}$$

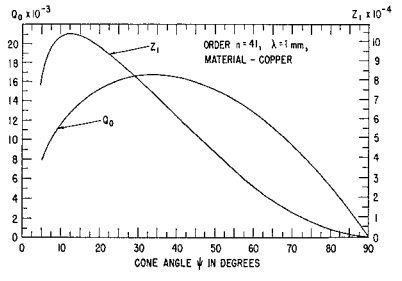

Fig. 6—Unloaded Q values and shunt impedance Z_i of biconical spherical resonator.

Values of Z_i ranging from 75,000 to 100,000 Ω are thus obtained for $n=41$, the diameter of the resonator at $\lambda=1$ mm then being 2 cm. The Q values are also relatively high for this wavelength, ranging up to 16,000. For a klystron resonator, Z_i is the important parameter and must be as high as possible. For other applications a higher Q may be required, and can be obtained by increasing n. Thus for $n=101$ and $\psi=22.5°$, we obtain $Q_0=34{,}200$ and $Z_i=83{,}500$ ohms, with a resonator diameter of 5 cm. The DX 151 Philips klystron for 4 mm wavelengths uses a conventional resonator of diameter 1.6 mm, and height 0.7 mm with a value of Z_i around 77,000 ohms.[13] Such a resonator would thus be extremely small at $\lambda=1$ mm, and Z_i would be reduced to around 38,000 ohms. The advantages of the biconical resonator are thus apparent.

Further computations for $\lambda=0.1$ mm, and $n=401$ are shown in Table II; here the increase in Q should be noted, values of 39,000 now being possible. Due to the increase in R_m at higher frequencies, Z_i decreases but even at $\lambda=0.1$ mm values around 24,000 ohms seem possible. The diameter of this resonator would again be around 2 cm at a sub-mm wavelength of 0.1 mm, an extremely important consideration for many areas of work.

TABLE II

VARIATION OF Q VALUES AND SHUNT IMPEDANCE Z_i FOR BICONICAL RESONATORS AT $\lambda=0.1$ MM AND ORDER OF INTERFERENCE $n=401$

ψ_0	10	13	22.5	33.5
Q_0	26,500	30,200	37,000	39,370
Z_i	24,100	24,400	22,300	17,600

For some purposes the resonator formed by a single re-entrant cone inside a hemisphere, as in Fig. 7, might be useful. Similar considerations apply to this type, and general expressions for Q_0 and Z_i are then

$$Q_0 = \frac{30\pi^2 n \log \cot (\psi/2)}{R_m[\log \cot (\psi/2) + P(\operatorname{cosec}\psi + 1)]}, \quad (12)$$

and

$$Z_i = \frac{7200\pi[\log \cot (\psi/2)]^2}{R_m[\log \cot (\psi/2) + P(1 + \operatorname{cosec}\psi)]}. \quad (13)$$

Both Q_0 and Z_i are thus smaller for this resonator, Z_i having around half the value for two re-entrant cones. However, such a resonator could be useful in applications where a number of closely spaced cavities are required.

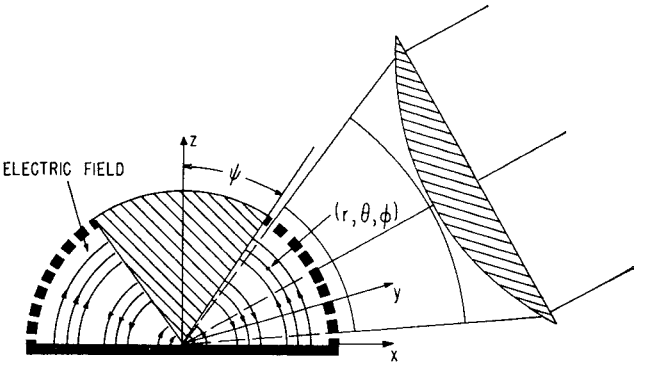

Fig. 7—Hemispherical conical resonator.

B. Coupling Considerations

Ideas on possible forms of coupling into such a resonator arise when it is considered as a distortion of the planar Fabry-Perot interferometer. Hence the design of the whole array of coupling holes will be similar, except now they will be on the surface of the spherical portion and focused radiation must be used as indicated in the figures. The intrinsic impedance of the principal mode is that of free space, *viz*, $E_\theta/H_\phi=\eta$, and the characteristic impedance Z_c may thus be regarded as derived from series and parallel combinations of elemental parallel-plate transmission lines, the number of which are determined by the hole spacings on the spherical surface. Since the number of such holes at fixed spacings around the circle $\theta=$constant on the sphere varies as $\sin\theta$, a resultant Z_c of the form given by (6) is obtained.

From such general considerations, we deduce that the impedance transformations through the equally spaced holes on the spherical surface are identical, since the electric and magnetic walls into which the cavity can be divided give rise to a system of equal parallel-plate transmission lines with intrinsic impedance η. The amplitude transmission coefficients are also identical for all such holes, and since the number of holes around a given latitude varies as $\sin\theta$, and the fields vary as $1/\sin\theta$, the total power transmission from the cavity is the same along each line of latitude. The holes can thus be equally spaced along circles of latitude; some adjustment of the final hole along such a circle will, however, be necessary in general. The same spacings in the θ direction may also be used, but the lines of hole centers need not coincide with lines of longitude.

[13] B. B. Van Iperen, "Reflex klystrons for millimeter waves," *Proc. Symp. on Millimeter Waves*, Polytechnic Inst. of Brooklyn, Brooklyn, N. Y., pp. 249–250; March, 1959.

The biconical resonator may be regarded as a transmission line of length $n\lambda/4$, and of characteristic impedance Z_c given by (6). The impedance across the cone apices for any uniform impedance Z_t over the spherical boundary is then given by

$$Z = Z_c \frac{Z_t + jZ_c \tan \beta l}{Z_c + jZ_t \tan \beta l}, \tag{14}$$

and for $l = n\lambda/4$, $Z = Z_c^2/Z_t$. For a coupling hole system extending over the complete spherical surface, Z_t will be uniform over the surface and may be deduced from the equivalent circuit for such a coupling hole. Thus, the load impedance at the apices can be determined, and hence the degree of loading as compared with the shunt impedance Z_t of the resonator can be deduced.

Another approach which is useful when only a part of the spherical surface has coupling holes, and also in the previous case, is to use the general formulas[7] to determine the Q factor and the shunt impedance Z_t. The impedances transformed from free space through such holes give rise to increased losses over that portion of the spherical boundary concerned, and the external Q values and load impedances can be determined. Thus the result for the increased power loss due to the load coupling will be given by

$$W_L = \tfrac{1}{2} R \int H_\phi H_\phi^* dA, \tag{15}$$

where the limits of integration for ϕ and θ extend over the coupling region on the sphere, and R is the resistive part of the load impedance at the spherical boundary. In this way the effect of various degrees of coupling can be considered and loaded Q values and load impedances determined. A number of coupling holes are thus required, and this approach should be reasonably valid if the area over which energy is coupled into or out of the resonator is large compared with the wavelength; otherwise diffraction effects will be serious. Since such resonators are intended for very short wavelengths this condition can be satisfied.

The coupling may thus be deduced from the equivalent circuit for a single coupling hole in a metal plate, which is shown in Fig. 8. Values of the susceptances are given by the following equations.[14]

$$B_a = \frac{B}{2Y_0} + \frac{|Y_0'|}{Y_0} \tanh\left(\frac{\pi t}{|\lambda_g'|}\right),$$

$$B_b = \frac{|Y_0'|}{Y_0} \operatorname{csch}\left(\frac{2\pi t}{|\lambda_g'|}\right), \tag{16}$$

where in our case $B/2Y_0 = (3a^2\lambda)/(2\pi D^3)$, and

$$\frac{|Y_0'|}{Y_0} = \frac{0.284 a_g^2 \lambda}{D^3}\left[1 - \left(\frac{1.706D}{\lambda}\right)^2\right]^{1/2}, \tag{17}$$

[14] N. Marcuvitz, "Waveguide Handbook," M.I.T. Rad. Lab. Ser., McGraw-Hill Book Co., Inc., New York, N. Y., pp. 408–412; 1951.

approximately. Here a_g refers to the large dimension of a rectangular waveguide propagating only the dominant mode, and $|\lambda_g'|$ is given in reference 14. For matched conditions in free space, the transformed normalized impedance at the inside wall of the sphere is then given by

$$Z = \frac{B_b^2 + j(B_a + B_b)(B_a^2 + 2B_aB_b + 1)}{(B_a^2 + 2B_aB_b)^2 + (B_a + B_b)^2}. \tag{18}$$

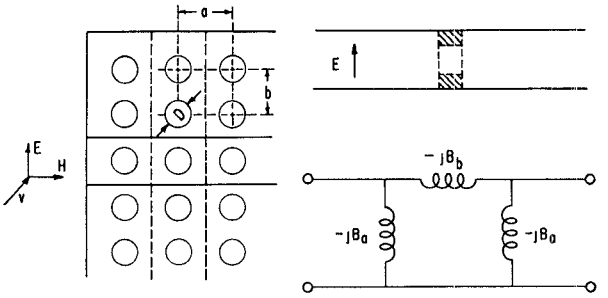

Fig. 8—Perforated metal plate and equivalent transmission line circuit electric wall ——, magnetic wall - - -.

The phase angle of the reflection coefficient at the spherical boundary may thus be determined, and the effect of transformed reactances on the resonance condition investigated for various hole configurations and wall thicknesses. This is important since the resonance condition demands a uniform phase shift over the spherical surface, and the phase changes occurring in regions where there are coupling holes differ from those at a metal wall. However, the phase change for holes in thick walls is not very different from that due to holes in the thinner walls where coupling is effected. This occurs because all holes are circular waveguides excited beyond cut-off, and the reactive contribution to the transformed impedance is close to that due to the hole at the inner surface of the sphere.

Thus, areas other than those used for energy transfer could possibly have thicker walls with holes similar to those in coupling areas. It may also be possible by suitable impedance transformations to have holes only in such coupling regions, with the remaining parts of the metallic spherical surface undisturbed. This would be a more satisfactory arrangement, and while the problem of coupling requires experimental evaluation, it seems clear that it can be done along the lines described.

Higher-Order Modes

So far, we have tacitly assumed the existence of only the principal mode in the biconical resonator, and we must now consider whether difficulties can arise from the higher-order modes which can also exist in it. The problem has been extensively treated by Schelkunoff in his work on antennas.[8] With an impressed RF voltage between the apices of the cones, the modes in question are the transverse magnetic spherical ones with $H_r = 0$.

As we have seen, in the biconical region a principal TEM wave exists with the electric field lines terminating normally to the conical surfaces. A continuation of this mode into free space is not possible, and in the case of the biconical antenna, other modes are generated at the spherical boundary between free space and the ends of the cone. The boundary conditions at the spherical boundary between the fields in the antenna region and the fields of spherical TM waves in free space may then be satisfied. Fig. 9 shows the electric field configuration for the first-order TM spherical wave in free space and in the biconical region respectively. The field patterns are quite similar, the difference being the presence of the small loops near the conical conductors which satisfy the boundary conditions for the electric field. The patterns for modes of higher-order are quite similar, except that the number of loops increases. Such field configurations are directly analogous to the electric field patterns of higher-order TM_{0n} modes between parallel plates and arise from appropriate distortions of such plates. If b is the spacing between the plates, the cut-off wavelengths for these modes are given by $2b/n$.

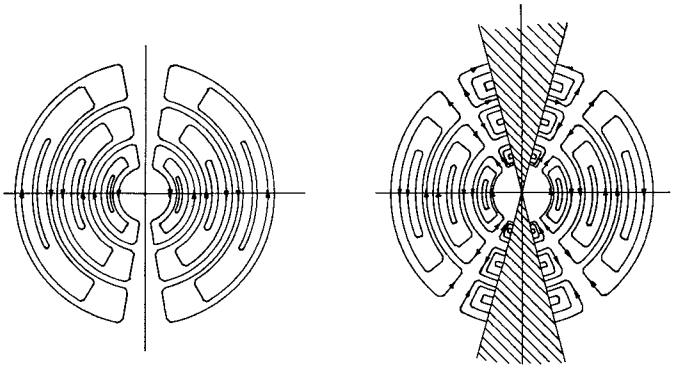

(a) (b)

Fig. 9—Electric field of first order TM spherical wave. (a) In free space. (b) With conical conductors. Magnetic lines circles coaxial with cones.

In the proposed biconical resonator, the fields are enclosed by a metallic spherical boundary on which the boundary conditions on the field may be satisfied by the fields of the dominant TEM wave, the electric field of which is given by

$$E_\theta = j\eta \frac{I_0 \sin \beta(l - r)}{2\pi r \sin \theta}, \tag{19}$$

where I_0 is the maximum current at $r=l$, and l is the radius of the sphere.[8] Thus, no higher-order modes arise at such a boundary, and this is still true when the coupling holes are present since these are spaced less than $\lambda/2$ apart. The fringing fields at the holes then correspond to non-propagating modes between parallel plates and represent a localized impedance at the spherical boundary. It follows then that no higher-order modes should exist in the resonator when the radius of the input region r_i is very small, or when the cones are pointed. Such higher-order modes may be generated in the input region around the apices of the cones if this is finite in extent, and this must be considered.

Expressions for such fields are given by Schelkunoff[8] and are independent of the angle ϕ. We shall be concerned with θ component of the electric field, which is given by

$$rE_\theta = \frac{\eta V(r)}{2\pi Z_c \sin \theta} + j\frac{\eta}{2\pi}\sum_n \frac{1}{n(n+1)}\frac{d}{d\theta} M_n(\cos\theta) S_n'(\beta r). \tag{20}$$

Here $M_n(\cos\theta) = \frac{1}{2}[P_n(\cos\theta) - P_n(-\cos\theta)]$, P_n being the Legendre function of order n, and

$$S_n(\beta r) = A_n Jn_n(\beta r) + B_n Nn_n(\beta r), \tag{21}$$

where $Jn_n(\beta r)$ and $Nn_n(\beta r)$ are the normalized Bessel functions of the first and second kind, and A_n and B_n are constants determined from the boundary conditions. Values of n over which the summation in (20) is made are determined by the relation

$$M_n(\cos\psi) = 0, \tag{22}$$

which corresponds to the condition $E_r = 0$ on the conical surfaces. Generally, the values of n are not integral and may be determined from the formula[8]

$$n_m(\psi) = \left[\left(\frac{2m\pi}{\pi - 2\psi}\right)^2 - \frac{1}{4}\right]^{1/2} - \frac{1}{2}, \tag{23}$$

where $m = 1, 2, 3, \cdots$.

The component E_θ of the electric field must vanish at the spherical boundary for all values of θ, and hence from (20) we must have

$$S_n'(\beta l) = 0, \tag{24}$$

expressing the resonance condition for any higher-order mode. For perturbations of the input region around the cone apices, the field at a specific input radius r_i may be expanded in terms of the orthogonal properties of Legendre functions and their derivatives; to obtain

$$E_n = \frac{\int_\psi^{\pi-\psi} r_i E_\theta(r_i) \sin\theta \frac{d}{d\theta}(M_n \cos\theta) d\theta}{\int_\psi^{\pi-\psi} \sin\theta \left[\frac{d}{d\theta} M_n(\cos\theta)\right]^2 d\theta}, \tag{25}$$

where

$$[j\eta S_n'(\beta r_i)]/[2\pi n(n+1)] = E_n. \tag{26}$$

The values of the constants A_n and B_n in (21) are now determined from (24) and (26) and will be small if the radius r_i is small. Hence for pointed cones in close proximity at the center, operation in the TEM mode without serious excitation of unwanted modes is feasible. This

also follows, because $Nn_n(\beta r_i)$ becomes infinite when $r_i \to 0$, and hence B_n must be zero in this case.

As an approximation to the resonance condition we may assume that $E_n = 0$ for small input regions or values of r_i. Then we find from (26) that

$$B_n/A_n = -J'n_n(\beta r_i)/N'n_n(\beta r_i), \tag{27}$$

and hence (24) becomes

$$J'n_n(\beta l)N'n_n(\beta r_i) - N'n_n(\beta l)J'n_n(\beta r_i) = 0. \tag{28}$$

But it follows from (27) that B_n/A_n tends to zero for small values of βr_i, particularly for large values of n. Hence for small perturbations of the input region, the resonance condition for higher modes is given by

$$J'n_n(\beta l) = 0, \tag{29}$$

and we have already noted that the amplitudes of such modes will also be small in this case. Such higher modes would also not exist if $r_i E_\theta(r_i) = 0$ for all θ, which occurs when the apices are joined by a metallic sphere in the input region. Other perturbations can be considered for specific cases, such as for a klystron type resonator, and would have to be investigated. The prime criterion is that the transition of the spherical fields of the TEM mode to those in the input region should be smooth and the field patterns matched as far as is possible. This can be approached by suitable shaping in such regions, and hence mode generation kept small.

Eq. (29) represents the condition for resonance in a higher-order mode, and for the large values of βl applicable here, we may write

$$Jn_n(\beta l) \simeq \sin(\beta l - n\pi/2),$$

and hence

$$J'n_n(\beta l \simeq \cos(\beta l - n\pi/2), \tag{30}$$

which gives the condition for resonance as

$$l = (2m + 1 + n)\lambda/4. \quad m = 1, 2, 3, \cdots. \tag{31}$$

Here n is not an integer in general, and this resonance condition can differ from that required for the principal mode. Thus even though higher-order modes are possible, depending on the shape of the input region between the cones, it may be possible to differentiate against them as regards resonance. We remark again that for small input regions, or perturbations, the amplitudes of such modes will be small and, in general, may be kept small by suitable transitions between the field regions in the resonator.

Conclusions

The basic ideas presented here appear to have considerable promise and significance for future work at mm and sub-mm wavelengths. Some results on a planar type of Fabry-Perot interferometer with high resolution may have already been given.[4] This interferometer represents the solution to the wavemeter problem for this wavelength region. The very high Q values already obtained at 6 mm wavelengths and the increases possible at very short wavelengths indicate its great potential use in all phases of millimeter-wave spectroscopy and maser research. A gaseous maser at a wavelength of 3.4 mm, using such an interferometer as the resonator, is under active development. Applications of this interferometer to solid state masers at sub-mm wavelengths are also feasible. As indicated, the curved reflector or focused type of Fabry-Perot interferometer may find similar applications at very short sub-mm or infrared wavelengths, and it represents an interesting problem for future investigation.

The new developments on the biconical spherical resonator which stem from the Fabry-Perot interferometer investigations appear quite significant. Suitable resonators are needed for electronic generation at mm wavelengths, for solid state masers at mm and sub-mm wavelengths, and for many other areas of research in this important wavelength region. The biconical resonator is a possible solution to this problem. The development of such a klystron resonator at reasonable orders of interference would materially help in the major problems of small size, circuit losses and heat dissipation in conventional resonators at these short wavelengths. There remains the problem of obtaining the required current densities from cathodes presently available, since the efficiency of electronic interaction with the resonator depends on the gap diameter as well as on the transit time across the gap.[13] However, the use of such a resonator would certainly assist in the generation of still shorter mm wavelengths, and would possibly permit greater ease in fabrication and greater power outputs to be obtained at wavelengths now possible. Higher-order modes in such a resonator have been discussed, and relatively mode-free operation should be possible. Further work must be done on the investigation of these, and on mechanical tuning methods.

In solid-state maser research this cavity represents a possible solution to the difficult problem of a resonator for a two-level, solid-state maser. This may well represent one method of obtaining relatively high-pulsed powers at mm and sub-mm wavelengths.[15] One of the major problems, that of obtaining a high Q cavity, appears to be adequately met by the biconical resonator, and for ideal conical geometries inside the sphere, mode troubles should not arise. Specimen shapes would conform to the field geometry at the cone apices or completely fill the cavity with the dc magnetic field suitably oriented along the axes of the cones, or along any other preferred direction. The proposed method of coupling would be extremely desirable in all such areas, since it would eliminate the necessity for long lengths of small waveguide into the low temperature bath. The Q of the cavity would also increase at low temperatures. Similar

[15] J. R. Singer, "Masers," John Wiley and Sons, Inc., New York, N. Y., pp. 71–87; 1959.

remarks apply to the three-level, solid-state maser.

Although further development of these resonators is required, such developments appear feasible in contrast to the present difficulties in applying conventional resonators to mm and sub-mm wavelengths. Such difficulties are very severe and most probably conventional resonators are impractical. There appears to be no reason why the ideas presented here should not be intensively pursued, as the rewards and knowledge to be gained from this virtually unexplored region of the electromagnetic spectrum are very great.

Note added in proof: The biconical spherical resonator has now been operated very satisfactorily by Dr. R. W. Zimmerer at wavelengths around 8 mm. The diameter of the sphere used was 4 inches, and the cone angle Ψ was 45°. Coupling holes after the manner described were used only in areas illuminated by the focused radiation. Both quarter-wavelength and half-wavelength resonances were observed and were the dominant ones. The Q value approaches the theoretical one, and higher mode effects are small.

ACKNOWLEDGMENT

The author would like to acknowledge the assistance and encouragement derived from discussions with his colleagues, and in particular, with Dr. R. C. Mockler.

A Recording Microwave Spectrograph*

D. ILIAS†, MEMBER, IRE, AND G. BOUDOURIS‡, SENIOR MEMBER IRE

Summary—**The principle of operation and the fundamentals of realization of a recording microwave spectrograph designed for use in the study of the absorption and the index of refraction of gases under medium pressures (1 mm Hg to 1 atm) are presented. The apparatus results from a similar spectrograph with synchroscope, in which the responses of the cavity resonators are interpreted by means of a pulse method. The high performances of the apparatus render its use advantageous, not only as a spectrograph, but also as an accurate recording refractometer, as well as a direct-reading Q-meter.**

I. INTRODUCTION

THE IDEA of the application of the pulse technique to microwave spectrographs with cavity resonators [12] was originally suggested in 1953 by Professor A. Gozzini of the University of Pisa (Italy) and his coworkers [2d]. Spectrographs of this type, although subject to continuous improvements, have been constructed in Pisa (Istituto di Fisica), in Paris (Laboratoire de Physique de l'Atmosphère) and in Amsterdam (Natuurkundig Laboratorium Universiteit). The new experimental setup has already been used successfully in various investigations [3]–[7].

The electronic indicator of this apparatus is an oscillograph used as a synchroscope. The result of the measurement is given by the relative positions of the pulses which appear on the screen of the synchroscope. In the following, we will refer to this apparatus as the "spectrograph with synchroscope."

The work described here makes use of this spectrograph to function as a recording instrument. As an output indicator, the synchroscope is replaced by an automatic recorder. The absorption coefficient or the index of refraction is recorded as a function of the pressure of the gas. The apparatus works, as does the previously mentioned spectrograph with synchroscope, in the centimetric (as well as in the millimetric) region of radio waves and is used in the study of gases under medium pressures (from about 1 mm Hg to 1 atm).

This function has been obtained through suitable modifications of the electronic parts of the instrument, especially those of the pulsers. The resulting recording spectrograph extends the possibilities of research in the field of microwave spectroscopy since it can also be used as a refractometer and as a Q-meter.

II. THE PRINCIPLE OF THE SPECTROGRAPH WITH SYNCHROSCOPE

The original spectrograph with synchroscope has been the subject of previous papers [2a], [5]. Briefly its principle is as follows.

The block diagram is shown in Fig. 1. The energy of the microwave source (a klystron) is frequency modulated by means of an isosceles triangular signal. The modulated energy is guided both to the channel of meas-

* Received by the PGMTT, August 4, 1960; revised manuscript received October 31, 1960.

† Laboratoire de Physique de l'Atmosphère, Faculty of Sciences, the Sorbonne Paris, France.

‡ Laboratoire de Spectroscopie Hertzienne, Faculty of Sciences, Sorbonne University, Paris, France. Formerly with Laboratoire de Physique de l'Atmosphère.